Laminar flame speed of ethanol/ammonia blends–An experimental and kinetic study

Pelé Ronan, Pierre Brequigny, Christine Mounaïm-Rousselle, Guillaume Dayma, Fabien Halter

Fuel Communications 10 (2022) 100052

Contents lists available at ScienceDirect

Fuel Communications

journal homepage: www.sciencedirect.com/journal/fuel-communications

Laminar flame speed of ethanol/ammonia blends–An experimental and kinetic study

Pelé Ronan [a,*], Brequigny Pierre [a], Mounaim-Rousselle Christine [a], Dayma Guillaume [b], Halter Fabien [b]

[a] 'Université d'Orléans, INSA-CVL, EA 4229 – PRISME, Orléans F-45072, France
[b] 'Université d'Orléans, CNRS-ICARE, Orléans, France

ARTICLE INFO

Keywords:
Laminar flame speed
Ethanol
Ammonia
Kinetic mechanisms

ABSTRACT

Blending bio-ethanol with ammonia is an interesting approach to reach carbon-neutrally combustion systems. As a fundamental parameter, laminar flame speed for different blends of ethanol/ammonia is explored using the spherical expanding flame technique under constant pressure conditions. A comparison to the few recent literature experimental results is proposed. An empirical correlation is developed to estimate the laminar flame speed of any ammonia/ethanol mixture as a function of the equivalence ratio at 1 bar and 423 K. Some simulation results are also provided to compare kinetics mechanisms accuracy to experimental data and identify the most relevant sensitive reactions. Two mechanisms are compared, one from the literature and another from the fusion of two mechanisms originally developed for pure ethanol and pure ammonia respectively. One major conclusion is that none of these mechanisms allows sufficient agreement with experimental data and more in-depth studies are still needed to provide high accurate kinetics mechanisms for ethanol/ammonia mixture. Sensitivity analysis highlights an important difference between the sensitive reactions with pure ammonia and ethanol blends. The key role of carbon reactions HCO(+*M*)<=>*H*+CO(+*M*) and CO+OH<=>CO_2+*H* on the laminar flame speed is shown for blends containing more than 50% of ethanol.

1. Introduction

Climate change has been one of the greatest challenges in the last decade and is unfortunately still an ongoing concern. Consequently, Europe has decided a drastic reduction of greenhouse gasses emission of 55% in 2030 compared to 1990 [1]. To take up this challenge, the share of renewable energy must reach at least 32% and the use of low carbon fuels and biofuels is necessary. Biofuels are highlighted as alternative energy sources and bio-ethanol is the most attractive one [2]. It can be produced from a wide variety of sources such as starch, sugarcane, lignocellulosic material derived from agricultural waste, and algae [3] reducing its CO_2 footprint. Bio-ethanol can be easily blended with gasoline with positive effects increasing engine efficiency [4] and decreasing dramatically CO and HC emissions [5].

Carbon-free fuels such as hydrogen and ammonia are also interesting solutions to decarbonize energy, transport, and industrial sectors, especially by considering their production from water electrolysis with green electricity. Hydrogen is an attractive energy carrier [6] but its storage issue, its low ignition energy, and very wide flammability range are the main drawbacks [7]. Ammonia, containing 17.8% by weight of hydrogen, can be stored in the liquid phase at approximately 9 bar at 20 °C or −34 °C at ambient pressure. Its high auto-ignition temperature and research octane number, narrow flammability range, and low laminar flame speed [8] are unfavorable combustion properties. Nevertheless, several studies have addressed the potential of ammonia as fuel in internal combustion engines, mainly blended with another fuel to promote ignition/combustion properties, as reviewed in Mounaïm-Rousselle and Brequigny [9] and Dimitriou and Javaid [10]. Recently, Lhuillier et al. [8] confirmed that ammonia/hydrogen is a suitable fuel for current spark-ignition engines with no design modifications. Other fuels can be blended with ammonia as bio-ethanol since it is considered carbon neutral. Indeed, bio-ethanol increases the reactivity of ammonia while remaining carbon-neutral fuel and can be safely stored in the liquid phase.

In most applications, laminar flame speed is a major property that drives the combustion process. The knowledge of the laminar flame

* Corresponding author.
E-mail address: ronan.pele@etu.univ-orleans.fr (P. Ronan).

https://doi.org/10.1016/j.jfueco.2022.100052
Received 22 November 2021; Received in revised form 21 January 2022; Accepted 26 January 2022
Available online 27 January 2022

speed is required to understand the burning behavior of an air/fuel mixture and is one key parameter to improve the validity of kinetic mechanisms. It needs to be provided as a function of the mixture itself, temperature, and pressure and can be measured by different experimental setups such as constant volume or pressure spherical chamber, heat flux method, counter-flow flame, etc.

Table 1 summarizes the experimental data of laminar flame speed, available in literature for pure ammonia and ethanol in similar conditions to this work. In the case of ethanol, several studies have measured its laminar flame speed in different conditions of pressure and temperature. As an example, Katoch et al. have [2] measured the laminar flame speed of ethanol/air mixture at 1 atm for a temperature range of 350–620 K and equivalence ratio of 0.7–1.3 using diverging channel method [16]. Broustail et al. [11] also measured ethanol/air laminar burning velocities at an initial temperature of 423 K, for equivalence ratio ranging from 0.7 to 1.4 and different initial pressures (0.1, 0.3, 0.5, and 1.0 MPa) using the spherical expanding flame methodology under constant pressure conditions. Both studies have suggested a correlation of laminar flame speed as a function of equivalence ratio, temperature, and pressure. Knorsch et al. [12] have compared the laminar flame speed of different gasoline alternative fuels such as ethanol at higher temperatures and also as a function of exhaust gas recirculation rates using the heat flux method. They found a good agreement with Broustail et al. [11].

In the case of ammonia, Hayakawa et al. [13] performed measurements at 298 K for different initial pressures (0.1, 0.3, and 0.5 MPa) and $0.7 \leq \Phi \leq 1.3$ using a constant pressure combustion chamber. Lhuillier et al. [14] measured NH_3/air flame speeds at atmospheric pressure and for temperatures ranging from 298 to 473 K. Due to extremely low values, around 8 cm s^{-1} at 298 K and 1 bar [14,15] compared to 45 cm s^{-1} for ethanol, for instance, in identical conditions, the addition of hydrogen in ammonia/air mixture to increase the laminar flame speed was also explored for example in Lhuillier et al. [14]. Some other studies investigated the oxy-combustion as Du et al. [15] to reach a maximum value of laminar flame speed around 125 cm s^{-1} at atmospheric pressure and 303 K. Mixing ammonia with other fuels such as methane [17,18], syngas [19], or DMM [20] is also explored but mixtures of ammonia and ethanol have received less attention [21].

The aims of the present work are: (1) to provide laminar flame speed values for different mixtures of ethanol/ammonia at 423 K and 1 bar using the spherical expanding flame technique under constant pressure conditions, (2) to compare these results with recent literature [21] and (3) to compare different kinetics mechanisms to the experimental data and propose an improved kinetic mechanism, based on the identification of the most sensitive reactions.

Table 1
Summary of experimental data available in literature for ethanol and ammonia laminar flame speed.

Fuel	T (K)	P (bar)	Φ	Technique	Reference
Ethanol	350–620	1.013	0.7–1.3	Diverging channel method	[2]
	423	1–10	0.7–1.4	Closed combustion vessel	[11]
	373–423	1	0.7–1.6	Heat flux	[12]
Ammonia	298	1–5	0.7–1.3	Closed combustion vessel	[13]
	298–473	1	0.8–1.4	Closed combustion vessel	[14]
Oxy-ammonia (0.6–1.0% O_2)	303	1.013	0.6–1.4	Closed combustion vessel	[15]

2. Experimental methods

2.1. Experimental set-up

The combustion chamber used is a stainless-steel spherical chamber with an internal volume of 4.2 L and an inner diameter of 200 mm as previously described in [14,22,23]. Four quartz windows of 70 mm diameter ensure optical access. The initial gasses are heated at 423 K thanks to a wire resistance located on the outer surface of the sphere. The vessel is emptied of gasses before any test by a vacuum pump until the pressure drops below 10 mbar. Ammonia is injected first, in the gaseous phase, by a flowmeter then, ethanol is injected, in the liquid phase, through a Coriolis mass flowmeter. Air is injected directly to the exit of the Coriolis flowmeter to push liquid ethanol in the pipe until the selected initial pressure. The inlet valve and intake pipe are heated to 423 K to ensure the vaporization of the liquid ethanol (vaporization temperature of 352 K at 1 bar). During the filling process, a fan is running to obtain a perfectly homogeneous premixed mixture and is stopped 10 s before ignition to avoid turbulent perturbations. Two tungsten electrodes of 0.5 mm and a distant of 1.5 mm, powered by a conventional capacitive discharge ignition system, initiate the ignition. The charging duration is set at 3 ms corresponding to 80 mJ of electrical energy, increased up to 5 ms for the conditions with the highest ratio of ammonia, due to ignition difficulties. The results displayed in the next sections are the averaged values of 5 identical tests with identical experimental conditions.

2.2. Optical technique

The Schlieren technique, based on the measurement of the deviation of the light source through the test section, is used to follow the flame front propagation. The Schlieren setup is presented in Fig. 1. The light from the LED (CBT120) is reflected in a parabolic mirror, with a focal of 800 mm, obtaining parallel beam. After the combustion chamber, the second parabolic mirror is used to focalize the light to the cut-off point. A set of two plano-convex lenses (focal length of 250 mm) is used to optimize the luminous signal on the camera sensor. The camera used is a High-Speed Phantom V1610, set to record from 8000 frames per second to 5000 fps for high ammonia contents. The resolution is 640 × 800 $pixels^2$ leading to a spatial resolution of 0.11 mm/pixel.

2.3. Image post-processing

MATLAB routines are used to post-process raw images (illustrated in Fig. 2) as described in the work of Di Lorenzo et al. [23]. The routine substrates background from images and then binarizes them using a specifically chosen threshold. This value depends on the natural chemiluminescence of the flame itself. Note that images are filtered using a low pass filter to smooth the contour and decrease noise.

The burnt gas area A is obtained from the contour determination and an equivalent flame radius R_f is calculated assuming a spherical flame geometry as:

$$R_f = \sqrt{\frac{A}{\pi}} \tag{1}$$

Minimum and maximum flame radii considered are respectively 6.5 and 25 mm as suggested in [24,25] to be unaffected by initial ignition deposit and confinement effects [23]. The flame speed S_b and stretch K can be deduced from the flame radius temporal evolution as:

$$S_b = \frac{dR_f}{dt}$$
$$K = \frac{2}{R_f}\frac{dR_f}{dt} \tag{2}$$

Using these two parameters, the unstretched laminar flame speed S_b^0

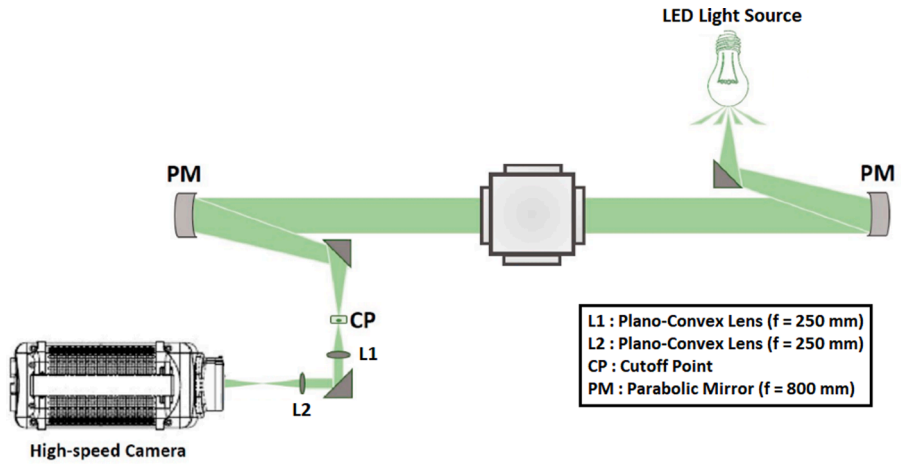

Fig. 1. Optical setup [22].

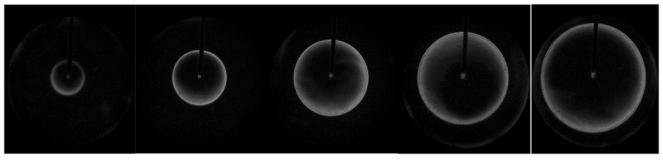

Fig. 2. Comparison of flames images 8 ms after ignition for the different blends from the left to the right $x_{C_2H_5OH} = 0,\ 0.25,\ 0.5,\ 0.75,\ 1.0$.

can be estimated through the non-linear quasi-steady extrapolation (3) proposed by Kelley and Law [25] and following the methodology described by Halter et al. [26].

$$\left(\frac{S_b}{S_b^0}\right)^2 ln\left(\frac{S_b}{S_b^0}\right)^2 = -\frac{2L_bK}{S_b^0} \tag{3}$$

L_b is the Markstein length which informs on the flame sensitivity to stretch effects. Finally, the unburned laminar flame speed S_u^0 is determined using the ratio of burned to unburned gas densities.

$$S_u^0 = \frac{\rho_b}{\rho_u} S_b^0 \tag{4}$$

The burned and unburned gas densities, ρ_b and ρ_u, are calculated by the premixed laminar flame-speed calculation module of ANSYS CHEMKIN-PRO [27] with the mechanism "Shrestha and PCRL" (see Section 4.2).

2.4. Experimental conditions

The laminar flame speed was measured at constant initial temperature and pressure of 423 K and 1 bar respectively. The ethanol/ammonia molar ratio in the fuel blend is defined as:

$$\begin{aligned} X_{C_2H_5OH} &= \frac{n_{C_2H_5OH}}{n_{C_2H_5OH} + n_{NH_3}} \\ n_{Fuel} &= n_{C_2H_5OH} + n_{NH_3} \end{aligned} \tag{5}$$

where n_{Fuel} is the mole number of the total fuel, composed of C_2H_5OH and NH_3. The equivalence ratio is defined following the global reaction:

$$n_{Fuel}\ Fuel + n_{air}\ Air = n_{CO_2}\ CO_2 + n_{H_2O}\ H_2O + n_{N_2}\ N_2 \tag{6}$$

considering 1 mole of $Fuel = X_{C_2H_5OH}\ C_2H_5OH + (1 - X_{C_2H_5OH})\ NH_3$

Therefore, the Equivalence Ratio (ER) is defined as:

$$\Phi = \left(\frac{n_{Fuel}}{n_{air}}\right) \Big/ \left(\frac{n_{Fuel}}{n_{air}}\right)_{stoichiometry} \tag{7}$$

Laminar flame speeds of ethanol/ammonia blends of $X_{C_2H_5OH} = 0.25$, 0.5 and 0.75 were determined at 423 K and 1 bar for Φ ranging from 0.8 to 1.3. The laminar flame speed values of pure ethanol and ammonia were taken from the work of Broustail et al. [11] and Lhuillier et al. [14]. obtained in identical conditions and setup. Note that measurements for stoichiometric pure ethanol and ammonia mixtures were repeated leading to less than 2% and 5% of difference in comparison with the previous study of Broustail et al. and Lhuillier et al. respectively.

2.5. Measurement uncertainties

Brequigny et al. [28] defined the uncertainty for the present setup as :

$$B_{S_l^0} = \sqrt{\left(\frac{\Delta S_u^0}{S_u^0}\right)_{P,T}^2 + \left(\frac{\Delta S_u^0}{S_u^0}\right)_{imaging}^2 + \left(\frac{\Delta S_u^0}{S_u^0}\right)_{statistical}^2} \tag{8}$$

Where the three terms represent experimental hardware, imaging, and statistical errors. Relative radiation-induced uncertainty can be important in case of extremely low laminar flame speed [14] nevertheless the laminar flame speed of blends are higher than 10 cm s^{-1}, conditions for which this uncertainty is negligible.

As the laminar flame speed can be expressed as $S_u^0 = S_{u,ref}^0 \left(\frac{T}{T_{ref}}\right)^{\alpha} \left(\frac{P}{P_{ref}}\right)^{\beta}$, the hardware error may be evaluated as:

$$\left(\frac{\Delta S_u^0}{S_u^0}\right)_{P,T} = |\alpha| \frac{\Delta T}{T} + |\beta| \frac{\Delta P}{P} \tag{9}$$

Where α and β are the temperature and pressure coefficients, depending on the fuel. The temperature of the mixture in the vessel is measured by a K-type thermocouple and can deviate up to 1%. A piezoelectric pressure transducer measures the pressure before ignition with a deviation of 2%. Considering the coefficient from ethanol $\alpha = 1.97$ [2] and $\beta = -0.284$ [11] due to the lack of information about the coefficients for the blends, the hardware error is estimated with Eq. (9) which is dependent on the temperature and pressure coefficients α and β. These coefficients are related to the fuel type itself. From the recent work of Kanoshima et al. [29],2 and -0.3 values were obtained for ammonia very similar to the ethanol case.

The global imaging error was estimated by Bréquigny et al. [28] to be 2.5% for the same experimental setup. The statistical error varies between 1% and 5% for blends.

Consequently, the uncertainty $B_{S_u^0}$ varies between 4% and 5% for blends.

Error bars are not plotted to have clear and readable figures but can be found in the supplementary material.

3. Kinetic modeling

Numerical simulations are carried out using the premixed laminar flame-speed calculation module of ANSYS CHEMKIN-PRO [27] with an average number of 1000 meshes on a 10 cm grid, a curvature of 0.1, and a gradient of 0.05 with 5 continuations. The laminar flame speed was calculated for $0.7 \leq \Phi \leq 1.4$ by 0.05 of increment.

Several recent ammonia kinetic mechanisms have been appraised: Tian et al. [30], Shrestha et al. [31], Stagni et al. [33], Otomo et al. [34] and compared to experimental measurements. The same comparison has been done with several ethanol kinetic mechanisms: NUI Galway [35], Polimi [36], PCRL [37], and Leplat et al. [38]. The mechanism of Wang et al. [21] developed for the blends of ethanol and ammonia was also tested.

4. Results and discussion

4.1. Comparison to literature data

Wang et al. [21] provided data on the laminar flame speed of ammonia/ethanol mixtures with $X_{C_2H_5OH} = 0.2, 0.4, 0.6, 0.8, 1.0$ at different temperatures 298, 348, 398 and 448 K using the heat flux method. They also developed a new kinetic mechanism.

Fig. 3.a compares the laminar flame speed of pure ethanol from Broustail et al. [11], Knorsch et al. [12], and Wang et al. [21]. Data from Wang et al. at 398 K are very close to Broustail et al. values (423 K) while a difference of 25 K separates these experiments. Values from the study of Knorsch et al. [12] show the same results as Broustail et al. [11] but their experimental values obtained at 373 K are similar to that of Wang et al. obtained at a temperature 25 K lower. Fig. 3.b presents the different ethanol laminar flame speed obtained at 373 K and 1 bar but with two different experimental set-ups: a closed combustion vessel (CCV) and a heat flux burner (HF). Rau et al. [39] studied the influence of the method on the laminar flame speed of ethanol/air and a difference of up to 5 cm s^{-11} is observed between both methods from their work in the same conditions. They compared their results to those from Varea et al. [37] obtained in a closed combustion vessel and those from Knorsch et al. [12] with a heat flux burner. A difference of up to 2.5 cm s^{-1} and 5 cm s^{-1} respectively for each method is obtained between their work and the literature. The maximum difference between all values is 8 cm s^{-1} at stoichiometric condition, Knorsch et al. being the lowest. These differences can result from the experimental set-up and the measurement technique, and the calculation of the density ratio itself as underlined by [39]. To go further, a simulation with Leplat et al. [38] mechanism at 398 K and 423 K shows a difference of 7.0 cm s^{-1} (see Table 2); a similar variation due to the methods is highlighted in Fig. 3.b.

Wang et al. [21] used a controlled evaporator mixer warmed at 473 K [40] to vaporize ethanol but this temperature is warmer than the unburned temperature and may overheat the reactive mixture. Furthermore, Wang et al. [21] recomposed air with two tanks of N2 and O2 without mentioning the ratio [40] while in this study, synthetic air contains 20.9% of O2. A variation of O2 content in air as 21%± 0.5% at 398 K and 1 bar changes the laminar flame speed predicted by Leplat et al. [38] mechanism by 6.7 cm s^{-1} (see Table 1). These differences in unburned temperature, air composition, and set-up between both studies can notably impact the laminar flame speed values.

Fig. 4 compares results obtained in this work with those of Wang et al. [21], although temperature and mixture ratio ranges are different. However, due to the similarity between pure ethanol data from Broustail et al. and Wang et al. at 398 K, shown in Fig. 2, these data at this temperature are compared to the present work at 423 K. The behavior of the laminar flame speed between both studies is similar. Values for 25% and 75% are very close to the data for 20% and 80% of Wang et al. The values obtained for blend of 50% in this work are well located between the values of 40% and 60% from Wang et al. The highest laminar flame speed is obtained for an equivalence ratio of 1.05–1.1. An addition of 25% of ethanol doubles the laminar flame speed of ammonia while the

Table 2
Comparison of laminar flame speed from Leplat et al. [38] mechanism at an equivalence ratio of 1.1 at 423 K and 398 K and different oxygen content.

Inlet temperature	02%	Laminar flame speed [cm s^{-1}]
423K	21%	72.4
398K	21%	65.4
	21.5%	68.6
	20.5%	62.1

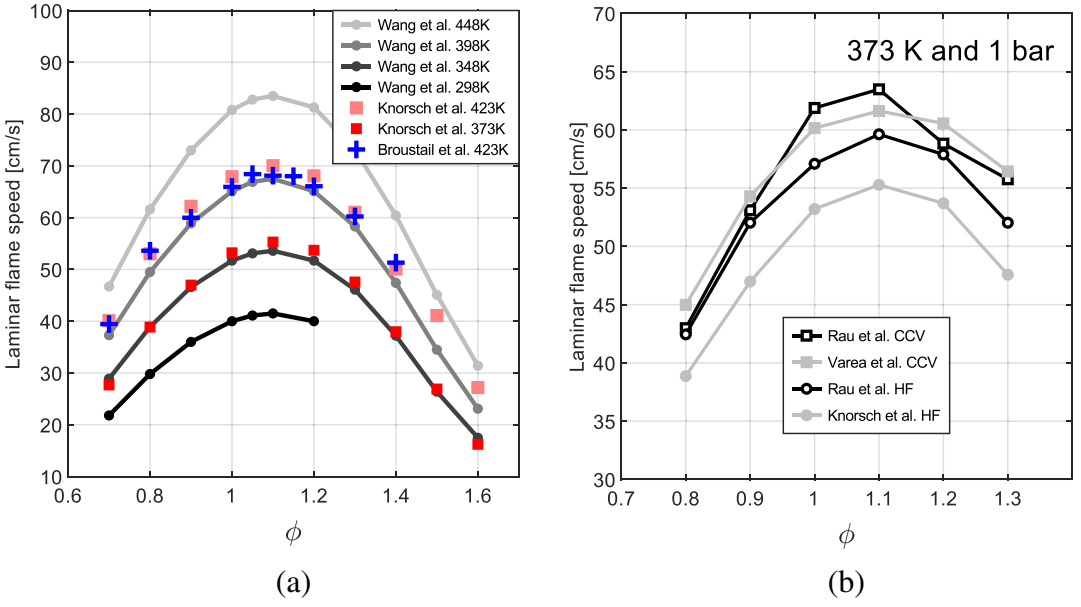

Fig. 3. Comparison of different experimental laminar flame speed values of ethanol/air mixtures from literature (a) at different ambient temperatures and (b) at 373 K with different experimental set-ups (CCV–Closed combustion vessel (square symbols) and HF–Heat flux technique (circles symbols)). All data obtained at 1 bar.

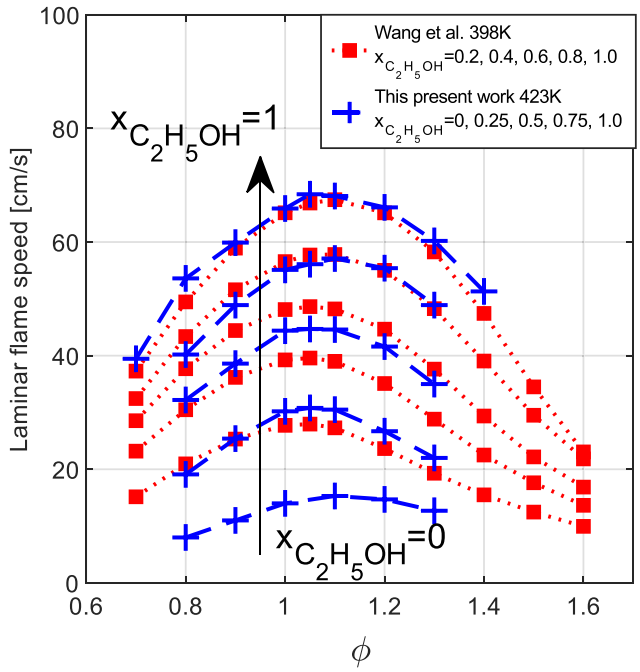

Fig. 4. Comparison between the experimental laminar flame speed values (+ and dashed line) of different ammonia/ethanol mixtures and those from Wang et al. (square and dotted line)–from the bottom to the top–$x_{C_2H_5OH} = 0$ up to $x_{C_2H_5OH} = 1$.

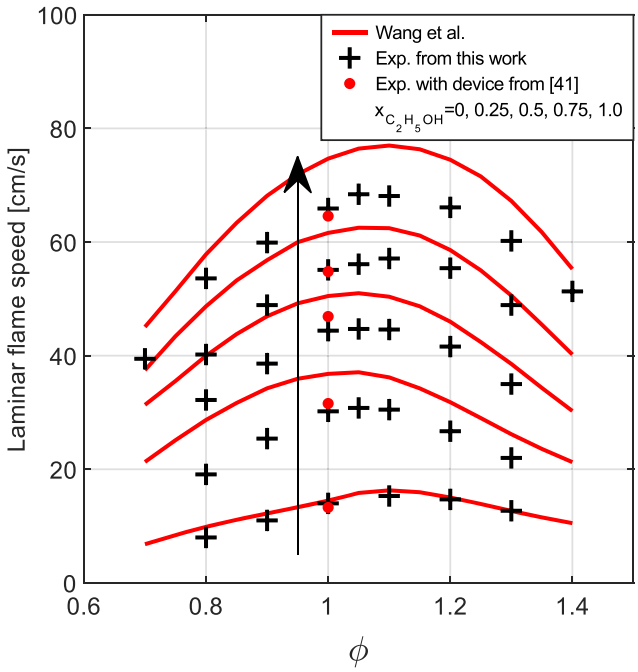

Fig. 5. Comparison of the laminar flame speed for different ammonia/ethanol mixtures from the kinetic simulation with Wang et al. mechanism (continuous line) and present experimental data (plus and circle symbols) at 423 K and 1 bar. $x_{C_2H_5OH} = 0,\ 0.25,\ 0.5,\ 0.75,\ 1.0$.

addition of 25% NH3 in ethanol decreases the laminar flame speed of ethanol by 15%.

Unfortunately, 100% ammonia values are not provided by Wang et al. and thus cannot be compared.

New results were carried out at the stoichiometric ratio, 423 K and 1 bar using the same constant pressure methodology with the constant-volume combustion chamber fully described in Halter et al. [41], with another injection device. Those new results based on a different injection method and chamber characteristics but with a similar constant pressure methodology aim to confirm the results found with the chamber described in 2.1.

Fig. 5 compares the results predicted by the kinetic mechanism developed by Wang et al. [21] to current results at 423 K and 1 bar and those obtained in the CVCC. The results from both experimental set-ups are very similar but the kinetic mechanism overestimates the laminar flame speed mainly due to the difference in the laminar flame speed for 100% ethanol between both studies. The agreement between the present experimental results and the calculations obtained from the mechanism of Wang et al. is not satisfactory and a new kinetic mechanism is required to obtain a better agreement.

4.2. Development of a new kinetic mechanism

The development of the new kinetic mechanism is based on the fusion of two mechanisms, one for pure ethanol and one for pure ammonia with the help of CONVERGE CFD 'Chemistry Tools'. The first step is to select the best mechanisms for 100% ethanol and 100% ammonia by comparison to our experimental data. The second step is to merge these mechanisms and verify how they predict the experimental data for pure ethanol and ammonia. The last step consists in verifying the prediction for different ethanol/ammonia blends and performing a sensitivity analysis.

4.2.1. Validation of mechanisms for pure ethanol and pure ammonia

The kinetic mechanisms were compared to experimental data of Lhuillier et al. [14] and Broustail et al. [11] for pure ammonia and ethanol mixtures respectively as shown in Figs. 6.a and 6.b.

The predicted results from the kinetics simulation of ammonia/air mixture are globally in good agreement with the experimental data, especially on the fuel-lean side. The maximum flame speed predicted by all mechanisms is around the equivalence ratio of 1.1; the highest and lowest value are respectively obtained with Tian (17.3 cm s^{-1}) and Otomo mechanisms (13.5 cm s^{-1}). For fuel-lean and stoichiometric conditions, Shrestha et al. mechanism is the most accurate, as displayed in Table 3, while the largest relative difference is obtained with Wang et al. and Tian et al. mechanisms. In fuel-rich conditions, Stagni et al. and Wang et al. mechanisms are in better agreement compared to Tian et al. and Otomo et al. mechanisms. Therefore, the most adapted mechanisms to provide accurate laminar flame speeds of ammonia/air mixtures with less than 10% of the relative difference are from Shrestha et al. and Stagni et al. .

All mechanisms overestimate the laminar flame speed for pure ethanol and Leplat et al. mechanism is the closest to the experimental data, as shown in Table 4 (less than 10% of relative difference). The values from PCRL mechanism are close to experimental data on the fuel-lean side but diverge on the rich side. Polimi and NUI Galway mechanisms provide the most different values for lean, rich, and stoichiometric conditions.

In the rest of the study, Tian et al. and NUI Galway mechanisms will not be considered.

4.2.2. Validation of a merged mechanism for pure component

Mechanisms merging was carried out using CONVERGE CFD 'Chemistry Tools'. The first mechanism is considered as the master and the second one is the donor. The merged mechanism receives all species and reactions of the master mechanism with their thermodynamic and kinetic parameters. Then, the merge mechanism is completed by the species and reactions from the donor, not present in the master thus meaning that, in case of duplicates, the master mechanism prevails. Depending on the role, master or donor, the merged mechanism can differ due to possible thermodynamic and kinetic differences between the similar species and reactions. This process can produce easily a new

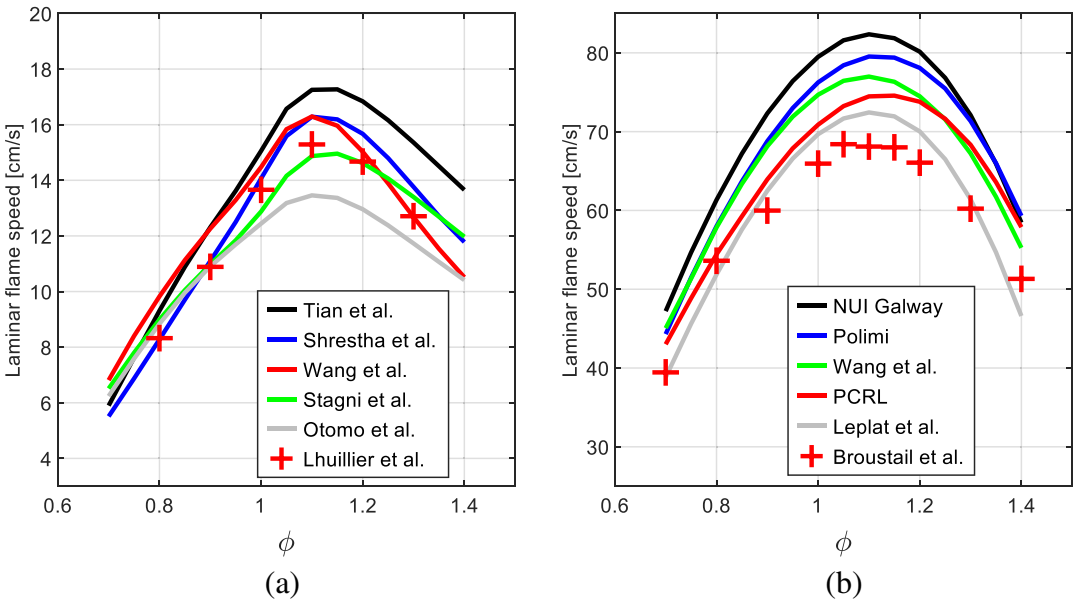

Fig. 6. Comparison of the laminar flame speed as a function of equivalence ratio between simulated values (lines) and experimental data (symbols) at 423 K and 1 bar, (a) pure ammonia and (b) pure ethanol.

Table 3
Comparison of relative differences between simulated values with different ammonia mechanisms and experimental values.

Φ	Tian et al.	Shrestha et al.	Wang et al.	Stagni et al.	Otomo et al.
0.8	12%	−1%	18%	8%	6%
1.0	10%	3%	5%	−6%	−9%
1.2	15%	7%	2%	0%	−12%

Table 4
Comparison of the relative difference between data from ethanol mechanisms and experimental values.

Φ	NUI Galway	Polimi	Wang et al.	PCRL	Leplat et al.
0.8	14%	8%	7%	2%	−3%
1.0	21%	16%	12%	7%	6%
1.2	21%	18%	12%	12%	6%

kinetics mechanism for fuel blends, but it still needs to be validated by using experimental data and possible modifications afterward to optimize it.

Many merges were done and the resulting mechanisms named "Master and Donor" were first compared to pure ammonia and ethanol experimental flame speeds as presented in Fig. 7.

Depending on the role of ethanol or ammonia mechanisms to generate the merged mechanism, calculations are completely different. For instance, the "Leplat and Shrestha" mechanism (blue full line in Fig. 7.a and b) is far from the experimental ammonia flame speeds (see Fig. 7.a) while the "Shrestha and Leplat" mechanism (blue full line in Fig. 7.c and d) provides very good agreement with pure ammonia flame speeds (see Fig. 7.c). The merged mechanism with the ammonia mechanism as master seems indifferent to the ethanol sub-mechanism as the donor for pure ammonia flame speed as illustrated in Fig. 6.c. In fact, the merged mechanisms with the ammonia mechanism as master received the same mechanism of oxidation of ammonia, and only carbon reactions are added from the donor, i.e. the ethanol mechanism. Almost the same behaviors, as seen in Fig. 7.b, can be noticed when considering the ethanol mechanism as master for pure ethanol results. However, the Shrestha mechanism contains sub-mechanisms of carbon species contrary to Stagni and Otomo ones. In fact, the Shrestha mechanism can add carbon reactions to the ethanol mechanism and consequently change the laminar flame speed of the merged mechanism. This change in laminar flame speed values is visible with PCRL as master (see Fig. 7.b) and also with Leplat where "Leplat and Otomo / Stagni" are similar while "Leplat and Shrestha" differs. Only one merged mechanism, namely "Shrestha and PCRL" mechanism, allows to reproduce satisfactorily both ammonia and ethanol experimental values, as can be seen in Fig. 7.c and Fig. 7.d.

4.2.3. Validation of the merged "Shrestha and PCRL" mechanism for ethanol/ammonia blends and sensitivity analysis

The selected "Shrestha and PCRL" mechanism, obtained with Shrestha [32] as master and PCRL [37] as the donor, is used to calculate the laminar flame speed of ethanol/ammonia blends and, compare with our experimental data. This comparison is presented in Fig. 8, and globally, an overestimation of the ethanol/ammonia blends flame speed is observed but with a good trend in terms of equivalence ratio and ethanol content as well as a good agreement for pure ethanol and pure ammonia results.

A sensitivity analysis was done on the A-factor from the Arrhenius law to identify the first fifteen reactions which influence the laminar flame speed.

$$S_{A-factor} = \frac{\Delta S_u^0}{S_u^0} \Big/ \frac{\Delta A}{A} \tag{10}$$

SA-factor expressed as Eq. (10) is the sensitivity factor calculated for one reaction and one condition, S_l^u is the unburned laminar flame speed and A the pre-exponential factor in the Arrhenius law. A positive or negative sensitivity factor means that an increase of pre-exponential factor increases or decreases respectively the laminar flame speed.

From this sensitivity analysis, it can be observed that the influence of the reactions on the laminar flame speed changes as a function of the equivalence ratio and the ethanol/ammonia blend.

The fifteen most sensitive reactions also differ depending on the equivalence and ethanol ratio and Fig. 9 sums up and compares all these reactions at a stochiometric ratio. The most important reaction is $O_2+H<=>OH+O$ for all the cases and is most predominant for pure ammonia conditions. The interactions between carbon and nitrogen are not obvious because no direct reaction between carbon and nitrogen is identified. Okafor et al. [42] show that both chemistries interact through H, OH, and O radicals pool. The behavior with pure ammonia is completely

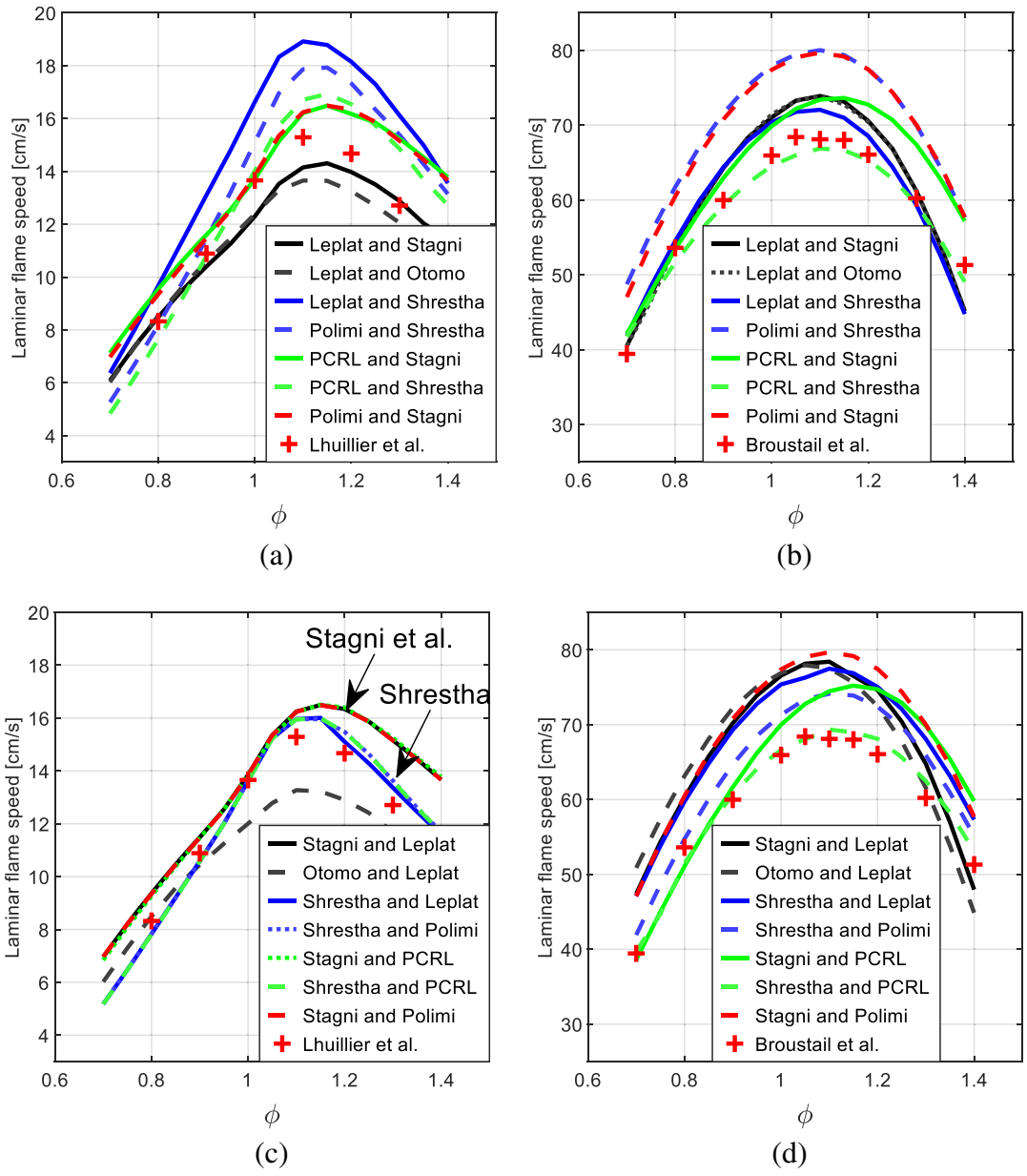

Fig. 7. Comparison of the laminar flame speed at 423 K and 1 bar as a function of equivalence ratio between ethanol (master) and ammonia (donor) merged mechanisms for (a) ammonia and (b) ethanol flames and ammonia (master) and ethanol (donor) merged mechanisms for (c) ammonia and (d) ethanol flames.

different: the sensitivity of reactions, $N_2H_2+M<=>NNH+H+M$ and $N_2H_2+H<=>NNH+H_2$, are important only with pure ammonia due to the high concentration of N_2H_2. Moreover, adding 25% of ethanol changes directly the sign of the sensitivity of reactions $O+OH+M<=>HO_2+M$ and $H+HO_2<=>2OH$ and decreases slightly the sensitivity of $H+O_2(+H_2O)<=>HO_2(+H_2O)$. However, the presence of HO_2 is remarkable in these three reactions. Focusing on the rate of production of HO_2 of these reactions, the forward step of $O+OH+M<=>HO_2+M$ and $H+O_2(+H_2O)<=>HO_2(+H_2O)$ for blends impact negatively the laminar flame speed due to consumption of H, O, OH radicals while the forward step $H+HO_2<=>2OH$ impact positively the laminar flame speed due to the OH production Fig. 9. However, in the case of ammonia, the reverse step $O+OH+M<=>HO_2+M$ impacts positively the laminar flame speed due to the formation of O and OH. The reaction $H+O_2(+H_2O)<=>HO_2(+H_2O)$ changes the sense of the reaction making the integrated consumption of H radical from this reaction almost insignificant and consequently without impact on the laminar speed. The forward step of $H+HO_2<=>2OH$ has a negative impact even with the production of OH but it can be due to the consumption of H radical which possibly more affects the ammonia combustion than OH.

The difference of behavior with pure ammonia is strongly influenced by HO_2 and can be one of the keys to better understanding the link between carbon and nitrogen chemistry.

$NH_2+NO<=>NNH+OH$, $HCO(+M)<=>H+CO(+M)$, $CO+OH<=>CO_2+H$, $NH_2+NH<=>N_2H_2+H$, and $NH_2+OH<=>NH+H_2O$ are the most important reactions for blends involving carbon and nitrogen and evolve non-linearly with the ethanol content. The sensitivities of carbon reactions are almost constant between $X_{C_2H_5OH}=0.5$ and $X_{C_2H_5OH}=1$ and higher for this range compared to nitrogen reactions. Nevertheless, the sensitivities of nitrogen reactions are directly in competition with carbon reactions or higher for low ethanol content up to 25%.

The study of Chen et al. [43] based on kinetic simulation with Wang et al. [21] mechanism identifies $O_2+H<=>OH+O$ as the major reaction and its impact decreases with the ethanol content. $CO+OH<=>CO_2+H$, $NH_2+NH<=>N_2H_2+H$ are also identified are the most important reactions and the same behavior with ethanol content is observed.

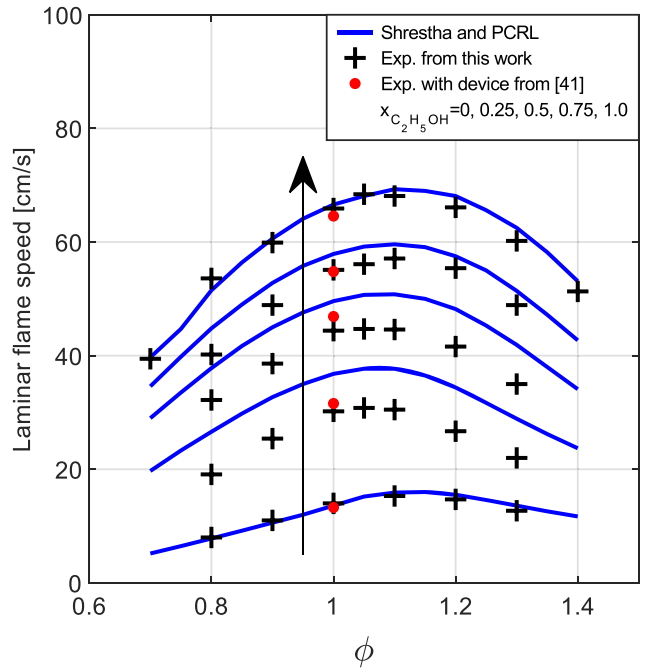

Fig. 8. Comparison of the laminar flame speed of different ammonia/ethanol blends from the kinetics simulation with Shrestha and PCRL merged mechanism (continuous line) and experimental data (+symbol) at 423 K and 1 bar–Bottom to top $X_{C_2H_5OH} = 0,\ 0.25,\ 0.5,\ 0.75,\ 1.0$.

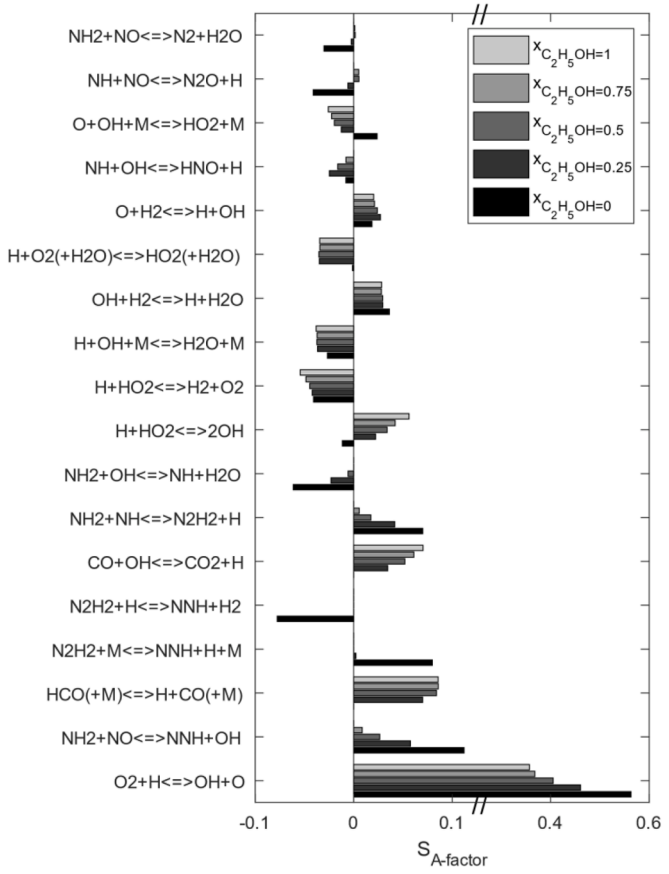

Fig. 9. Comparison of the $S_{A-factor}$ for the fifteen most important reactions for each ethanol/ammonia ratio (stoichiometric condition) with the kinetics simulation of Shrestha and PCRL mechanism.

However, some reactions as $N_2H_2+M<=>NNH+H + M$ and $N_2H_2+H<=>NNH+H_2$ are not defined in the Wang et al. mechanism consequently are not identified as important for ammonia.

Fig. 10 compares the principal normalized sensitivities of carbon and nitrogen reactions for blends. The evolution of the normalized sensitivities is not linear with the ethanol content; adding a small amount of ethanol in ammonia increases and decreases slightly the sensitivities of carbon and nitrogen reactions respectively while adding a small amount of ammonia in ethanol changes weakly the sensitivities.

Sensitivities of carbon reactions play a major role in laminar flame speed for blends higher than 50% of ethanol compared to the nitrogen reactions.

$S^0_{u\,Factor}$, as indicated by Eq. (11), is the flame speed increase (ratio of the laminar flame speed of a mixture of ammonia/ethanol over that of pure ammonia at the same equivalence ratio).

$$S^0_{u\,Factor} = \left.\frac{S^0_u\left(X_{C_2H_5OH}\right)}{S^0_u\left(X_{C_2H_5OH}=0\right)}\right|_{\Phi} \tag{11}$$

Fig. 11 shows the evolution of $S^0_{u\,Factor}$ as a function of the fuel mixture for all equivalence ratios. $S^0_{u\,Factor}$ increases linearly with $X_{c_2H_5OH}$ and consequently the laminar flame speed. $S^0_{u\,Factor}$ is more elevated for fuel-lean mixtures and decreases when the equivalence ratio increases until stabilization in the rich condition. The laminar flame speed for blends increases further compared to the laminar flame speed of ammonia in lean conditions compared to rich conditions.

4.2.2. *Validation of a laminar flame speed correlation depending on the equivalence and ethanol ratio*

A correlation was established based on the current experimental results (Eq. (12)).

$$S^0_u\left(\Phi, X_{C_2H_5OH}\right) = \beta - (\alpha - \Phi)^2 a \tag{12}$$

S^0_u is expressed as a parabola function dependant on the equivalence ratio. β, α and a are constant values that only depend on the ethanol ratio. They correspond to the maximum laminar flame speed "β" at the equivalence ratio "α" and "a" is the coefficient determining the gradient

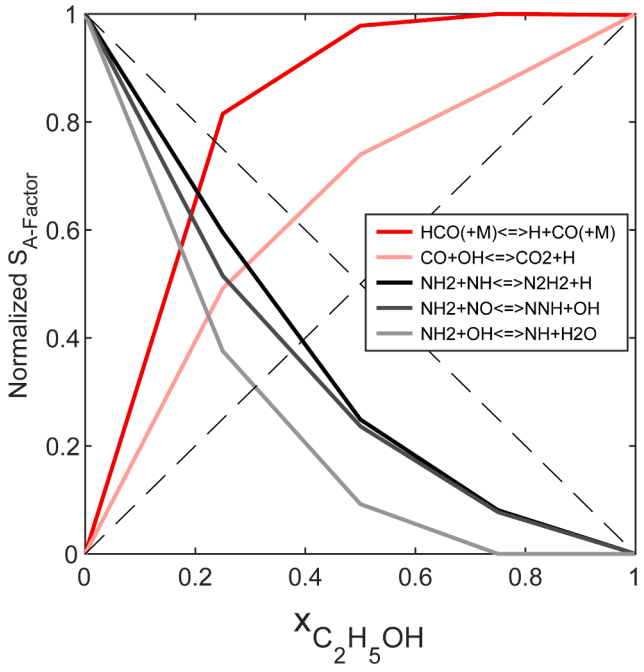

Fig. 10. Normalized $S_{A-factor}$ evolutions as a function of the ethanol content for the most important carbon and nitrogen reactions (stochiometric condition) for each ethanol/ammonia blend using the Shrestha and PCRL mechanism.

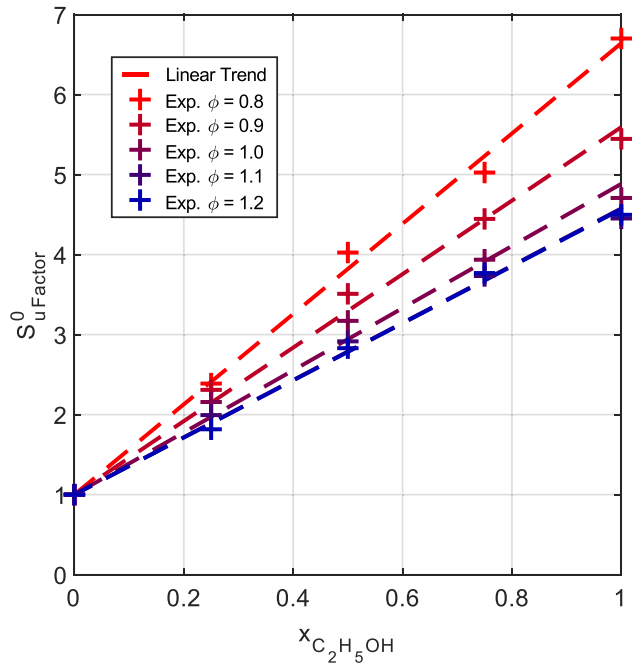

Fig. 11. Trend of the $S^0_{u\,Factor}$ as a function of the ethanol/ammonia blend ratio $X_{C_2H_5OH}$ and the equivalence ratio.

of the function.

The derivative of Eq. (12) with respect to the equivalence ratio is evaluated in Eq. (13).

$$\frac{\partial S_u^0}{\partial \Phi} = 2a(\alpha - \Phi) \tag{13}$$

$\frac{dS_u^0}{d\Phi}$ exhibits a linear trend as observed in Fig. 12 for $X_{C_2H_5OH} = 0.5$. The same conclusions are drawn for other fuel mixtures confirming the presupposed parabolic function for the laminar flame speed.

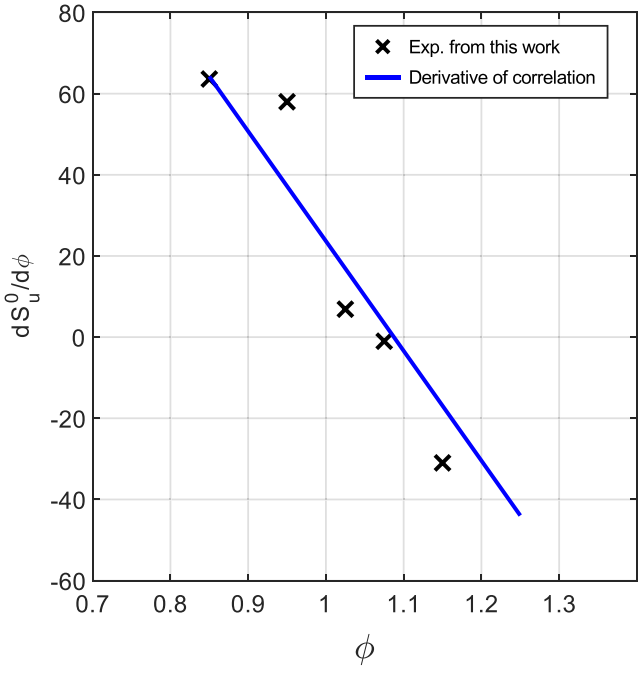

Fig. 12. $\frac{dS_u^0}{d\Phi}$ as a function of equivalence ratio for $X_{C_2H_5OH} = 0.5$. Black symbols for experimental results, blue continuous line for linear correlation. 423K and 1 bar.

The constants β, α and a were optimized by using an error minimization routine and are defined as:

$$\alpha = 0.015X_{C_2H_5OH} + 1.0772 \tag{14}$$

$$a = 25X^2_{C_2H_5OH} + 58X_{C_2H_5OH} + 100 \tag{15}$$

$$\beta = 52X_{C_2H_5OH} + 17 \tag{16}$$

Fig. 13 compares the correlation to the experimental data and a good agreement is found.

The correlation is optimized for one pressure/temperature condition but could be extended to other pressures and temperatures. Therefore, more experimental data at different temperature/pressure are still needed to improve this correlation and more globally, the dependence of pressure and temperature to the constants β, α and a should be found. The presupposed parabolic function should be verified for the other conditions.

5. Conclusion

For the first time, the laminar flame speed for different ethanol/ammonia blends (25%, 50%, and 75% in vol. of ethanol) for Φ ranging from 0.8 to 1.3 at 423 K, and 1 bar were measured with the spherical expanding flame technique under constant pressure conditions. When increasing the ethanol/ammonia ratio the laminar flame speed increases linearly with the ethanol content. The laminar flame speed of blends in lean conditions increases further compared to the laminar flame speed of ammonia in comparison in rich conditions. A comparison with Wang et al. exhibits a shift in the laminar flame speeds of ethanol. However, additional results performed with a different set-up confirm current experimental data. The values at 398 K from Wang et al. and those obtained in this work at 423 K show globally the same behavior.

A first step in developing a kinetic mechanism resulting from the fusion of two mechanisms was done. However, this new mechanism overestimates laminar flame speed data for blends and new experiments at different temperatures and pressures are needed to validate a new

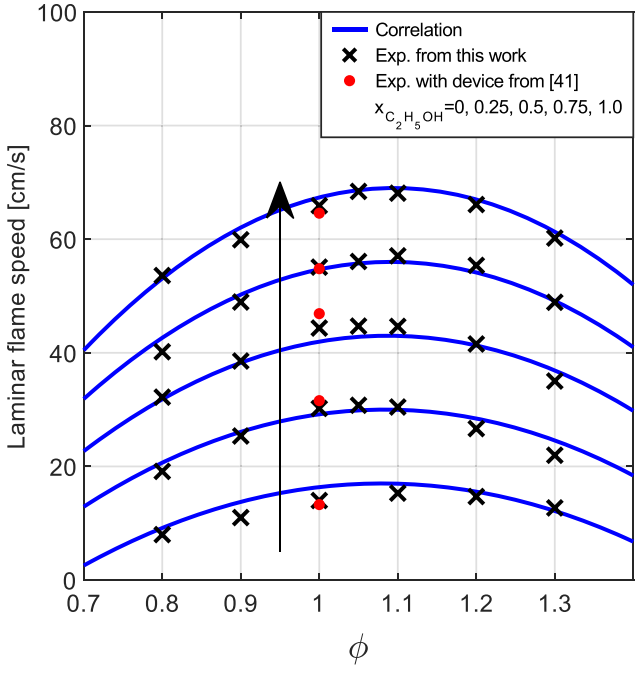

Fig. 13. Comparison of the laminar flame speed of different ammonia/ethanol blends. Blue continuous lines for the correlation. Black symbols for experimental results. 423 K and 1 bar. From bottom to top $X_{C_2H_5OH} = 0,\ 0.25,\ 0.5,\ 0.75,\ 1.0$.

mechanism. Sensitivity analysis highlights an important difference between the sensitive reactions for pure ammonia and blends; adding a small amount of ethanol changes suddenly the sensitive reactions. Sensitivity analysis shows that carbon reactions play a major role in ethanol ratios higher than 50%. The HO_2 is highlighted to be a specs influencing slightly the laminar flame speed sensibility of some reactions and can be one of the keys to understanding the link between carbon/nitrogen chemistry.

Future work will focus on the measurement of the laminar flame speed of ethanol/ammonia mixture at different temperatures and pressures to refine the kinetic mechanism in a wider range of conditions.

CRediT authorship contribution statement

Pelé Ronan: Writing – original draft. **Brequigny Pierre:** Writing – review & editing. **Mounaim-Rousselle Christine:** Supervision. **Dayma Guillaume:** Writing – review & editing. **Halter Fabien:** Writing – review & editing.

Declaration of Competing Interest

The authors declare that they have no known competing financial interests or personal relationships that could have appeared to influence the work reported in this paper.

Supplementary materials

Supplementary material associated with this article can be found, in the online version, at doi:10.1016/j.jfueco.2022.100052.

References

[1] 2030 climate & energy framework, (n.d.). https://ec.europa.eu/clima/policies/strategies/2030_fr.

[2] Katoch A, Millán-Merino A, Kumar S. Measurement of laminar burning velocity of ethanol-air mixtures at elevated temperatures. Fuel 2018;231:37–44. https://doi.org/10.1016/j.fuel.2018.05.083.

[3] Geddes CC, Nieves IU, Ingram LO. Advances in ethanol production. Curr Opin Biotechnol 2011;22:312–9. https://doi.org/10.1016/j.copbio.2011.04.012.

[4] Turner D, Xu H, Cracknell RF, Natarajan V, Chen X. Combustion performance of bio-ethanol at various blend ratios in a gasoline direct injection engine. Fuel 2011;90:1999–2006. https://doi.org/10.1016/j.fuel.2010.12.025.

[5] Hsieh WD, Chen RH, Wu TL, Lin TH. Engine performance and pollutant emission of an SI engine using ethanol-gasoline blended fuels. Atmos Environ 2002;36:403–10. https://doi.org/10.1016/S1352-2310(01)00508-8.

[6] V.T. Sacramento EM, Carvalho P, Lima LC. Feasibility study for the transition towards a hydrogen economy–A case study in Brazil Energy Pol 2013.

[7] Li Y, Bi M, Li B, Zhou Y, Huang L, Gao W. Explosion hazard evaluation of renewable hydrogen/ammonia/air fuels. Energy 2018;159:252–63. https://doi.org/10.1016/j.energy.2018.06.174.

[8] Lhuillier C, Brequigny P, Contino F, Mounaïm-Rousselle C. Experimental study on ammonia/hydrogen/air combustion in spark ignition engine conditions. Fuel 2020;269:117448. https://doi.org/10.1016/j.fuel.2020.117448.

[9] Mounaim-Rousselle C, Brequigny P. Ammonia as fuel for low-carbon spark-ignition engines of tomorrow's passenger cars. Front Mech Eng 2020;6:70. https://doi.org/10.3389/fmech.2020.00070.

[10] Dimitriou P, Javaid R. A review of ammonia as a compression ignition engine fuel. Int J Hydrogen Energy 2020;45:7098–118. https://doi.org/10.1016/j.ijhydene.2019.12.209.

[11] Broustail G, Halter F, Seers P, Moréac G, Mounaïm-Rousselle C. Experimental determination of laminar burning velocity for butanol/iso-octane and ethanol/iso-octane blends for different initial pressures. Fuel 2013;106:310–7. https://doi.org/10.1016/j.fuel.2012.10.066.

[12] Knorsch T, Zackel A, Mamaikin D, Zigan L, Wensing M. Comparison of different gasoline alternative fuels in terms of laminar burning velocity at increased gas temperatures and exhaust gas recirculation rates. Energy Fuels 2014;28:1446–52. https://doi.org/10.1021/ef4021922.

[13] Hayakawa A, Goto T, Mimoto R, Arakawa Y, Kudo T, Kobayashi H. Laminar burning velocity and Markstein length of ammonia/air premixed flames at various pressures. Fuel 2015;159:98–106. https://doi.org/10.1016/j.fuel.2015.06.070.

[14] Lhuillier C, Brequigny P, Lamoureux N, Contino F, Mounaïm-Rousselle C. Experimental investigation on laminar burning velocities of ammonia/hydrogen/air mixtures at elevated temperatures. Fuel 2020;263:116653. https://doi.org/10.1016/j.fuel.2019.116653.

[15] Wang D, Ji C, Wang Z, Wang S, Zhang T, Yang J. Measurement of oxy-ammonia laminar burning velocity at normal and elevated temperatures. Fuel 2020;279:118425. https://doi.org/10.1016/j.fuel.2020.118425.

[16] Konnov AA, Mohammad A, Kishore VR, Il Kim N, Prathap C, Kumar S. A comprehensive review of measurements and data analysis of laminar burning velocities for various fuel+air mixtures. Prog Energy Combust Sci 2018;68:197–267. https://doi.org/10.1016/j.pecs.2018.05.003.

[17] Okafor EC, Naito Y, Colson S, Ichikawa A, Kudo T, Hayakawa A, Kobayashi H. Measurement and modeling of the laminar burning velocity of methane-ammonia-air flames at high pressures using a reduced reaction mechanism. Combust Flame 2019;204:162–75. https://doi.org/10.1016/j.combustflame.2019.03.008.

[18] Xiao H, Valera-Medina A, Bowen PJ. Study on premixed combustion characteristics of co-firing ammonia/methane fuels. Energy 2017;140:125–35. https://doi.org/10.1016/j.energy.2017.08.077.

[19] Wang S, Wang Z, Elbaz AM, Han X, He Y, Costa M, Konnov AA, Roberts WL. Experimental study and kinetic analysis of the laminar burning velocity of NH_3/syngas/air, NH_3/CO/air and NH_3/H_2/air premixed flames at elevated pressures. Combust Flame 2020;221:270–87. https://doi.org/10.1016/j.combustflame.2020.08.004.

[20] Elbaz AM, Giri BR, Issayev G, Shrestha KP, Mauss F, Farooq A, Roberts WL. Experimental and kinetic modeling study of laminar flame speed of dimethoxymethane and ammonia blends. Energy Fuels 2020;34:14726–40. https://doi.org/10.1021/acs.energyfuels.0c02269.

[21] Wang Z, Han X, He Y, Zhu R, Zhu Y, Zhou Z, Cen K. Experimental and kinetic study on the laminar burning velocities of NH_3 mixing with CH_3OH and C_2H_5OH in premixed flames. Combust Flame 2021;229:111392. https://doi.org/10.1016/j.combustflame.2021.02.038.

[22] Rabello de Castro R, Brequigny P, Dufitumukiza JP, Mounaïm-Rousselle C. Laminar flame speed of different syngas compositions for varying thermodynamic conditions. Fuel 2021;301:121025. https://doi.org/10.1016/j.fuel.2021.121025.

[23] Di Lorenzo M, Brequigny P, Foucher F, Mounaïm-Rousselle C. Validation of TRF-E as gasoline surrogate through an experimental laminar burning speed investigation. Fuel 2019;253:1578–88. https://doi.org/10.1016/j.fuel.2019.05.081.

[24] Burke MP, Chen Z, Ju Y, Dryer FL. Effect of cylindrical confinement on the determination of laminar flame speeds using outwardly propagating flames. Combust Flame 2009;156:771–9. https://doi.org/10.1016/j.combustflame.2009.01.013.

[25] Kelley AP, Law CK. Nonlinear effects in the extraction of laminar flame speeds from expanding spherical flames. Combust Flame 2009;156:1844–51. https://doi.org/10.1016/j.combustflame.2009.04.004.

[26] Halter F, Tahtouh T, Mounaïm-Rousselle C. Nonlinear effects of stretch on the flame front propagation. Combust Flame 2010;157:1825–32. https://doi.org/10.1016/j.combustflame.2010.05.013.

[27] Kee RJ, Rupley FM, Miller JA. Chemkin-Ii–A fortran chemical kinetics package for the analysis of gas-phase chemical kinetics. J Chem Inf Model 1989;53:1689–99.

[28] Brequigny P, Uesaka H, Sliti Z, Segawa D, Foucher F, Dayma G. Uncertainty in measuring laminar burning velocity from expanding methane-air flames at low pressures, 11th Mediterranean. Combust Symp 2019:16–20.

[29] Kanoshima R, Hayakawa A, Kudo T, Okafor EC, Colson S, Ichikawa A, Kudo T, Kobayashi H. Effects of initial mixture temperature and pressure on laminar burning velocity and Markstein length of ammonia/air premixed laminar flames. Fuel 2022;310:122149. https://doi.org/10.1016/j.fuel.2021.122149.

[30] Tian Z, Li Y, Zhang L, Glarborg P, Qi F. An experimental and kinetic modeling study of premixed NH_3/CH_4/O_2/Ar flames at low pressure. Combust Flame 2009;156:1413–26. https://doi.org/10.1016/j.combustflame.2009.03.005.

[31] Shrestha KP, Seidel L, Zeuch T, Mauss F. Detailed kinetic mechanism for the oxidation of ammonia including the formation and reduction of nitrogen oxides. Energy Fuels 2018;32:10202–17. https://doi.org/10.1021/acs.energyfuels.8b01056.

[32] Shrestha KP, Lhuillier C, Barbosa AA, Brequigny P, Contino F, Mounaïm-Rousselle C, Seidel L, Mauss F. An experimental and modeling study of ammonia with enriched oxygen content and ammonia/hydrogen laminar flame speed at elevated pressure and temperature. Proc Combust Inst 2020;38:2163–74. https://doi.org/10.1016/j.proci.2020.06.197.

[33] Arunthanayothin S, Stagni A, Song Y, Herbinet O, Faravelli T, Battin-Leclerc F. Ammonia-methane interaction in jet-stirred and flow reactors–An experimental and kinetic modeling study. Proc Combust Inst 2021;38:345–53. https://doi.org/10.1016/j.proci.2020.07.061.

[34] Otomo J, Koshi M, Mitsumori T, Iwasaki H, Yamada K. Chemical kinetic modeling of ammonia oxidation with improved reaction mechanism for ammonia/air and ammonia/hydrogen/air combustion. Int J Hydrogen Energy 2018;43:3004–14. https://doi.org/10.1016/j.ijhydene.2017.12.066.

[35] Mittal G, Burke SM, Davies VA, Parajuli B, Metcalfe WK, Curran HJ. Auto-ignition of ethanol in a rapid compression machine. Combust Flame 2014;161:1164–71. https://doi.org/10.1016/j.combustflame.2013.11.005.

[36] E. Ranzi, A. Frassoldati, A. Stagni, M. Pelucchi, A. Cuoci, T. Faravelli, Reduced kinetic schemes of complex reaction systems–Fossil and biomass-derived transportation fuels, 2014. 10.1002/kin.20867.
[37] Roy S, Askari O. A new detailed ethanol kinetic mechanism at engine-relevant conditions. Energy Fuels 2020;34:3691–708. https://doi.org/10.1021/acs.energyfuels.9b03314.
[38] Leplat N, Dagaut P, Togbé C, Vandooren J. Numerical and experimental study of ethanol combustion and oxidation in laminar premixed flames and in jet-stirred reactor. Combust Flame 2011;158:705–25. https://doi.org/10.1016/j.combustflame.2010.12.008.
[39] Rau F, Hartl S, Hasse C. Numerical and experimental investigation of the laminar burning velocity of biofuels at atmospheric and high-pressure conditions. Fuel 2019;247:250–6. https://doi.org/10.1016/j.fuel.2019.03.024.
[40] Han X, Wang Z, He Y, Wang S, Liu Y, Konnov AA. Temperature dependence of the laminar burning velocity for n-heptane and iso-octane/air flames. Fuel 2020;276:118007. https://doi.org/10.1016/j.fuel.2020.118007.
[41] Halter F, Chen Z, Dayma G, Bariki C, Wang Y, Dagaut P, Chauveau C. Development of an optically accessible apparatus to characterize the evolution of spherically expanding flames under constant volume conditions. Combust Flame 2020;212:165–76. https://doi.org/10.1016/j.combustflame.2019.10.027.
[42] Okafor EC, Naito Y, Colson S, Ichikawa A, Kudo T, Hayakawa A, Kobayashi H. Experimental and numerical study of the laminar burning velocity of CH_4–NH_3–air premixed flames. Combust Flame 2018;187:185–98. https://doi.org/10.1016/j.combustflame.2017.09.002.
[43] Chen Z, Jiang Y. Kinetic modeling investigation on the NH_3/C_2H_5OH/air laminar premixed burning characteristics at different equivalence ratios. Energy Sources A Recover Util Environ Eff 2021;00:1–14. https://doi.org/10.1080/15567036.2021.1998253.